SUPPLEMENTARY INFORMATION
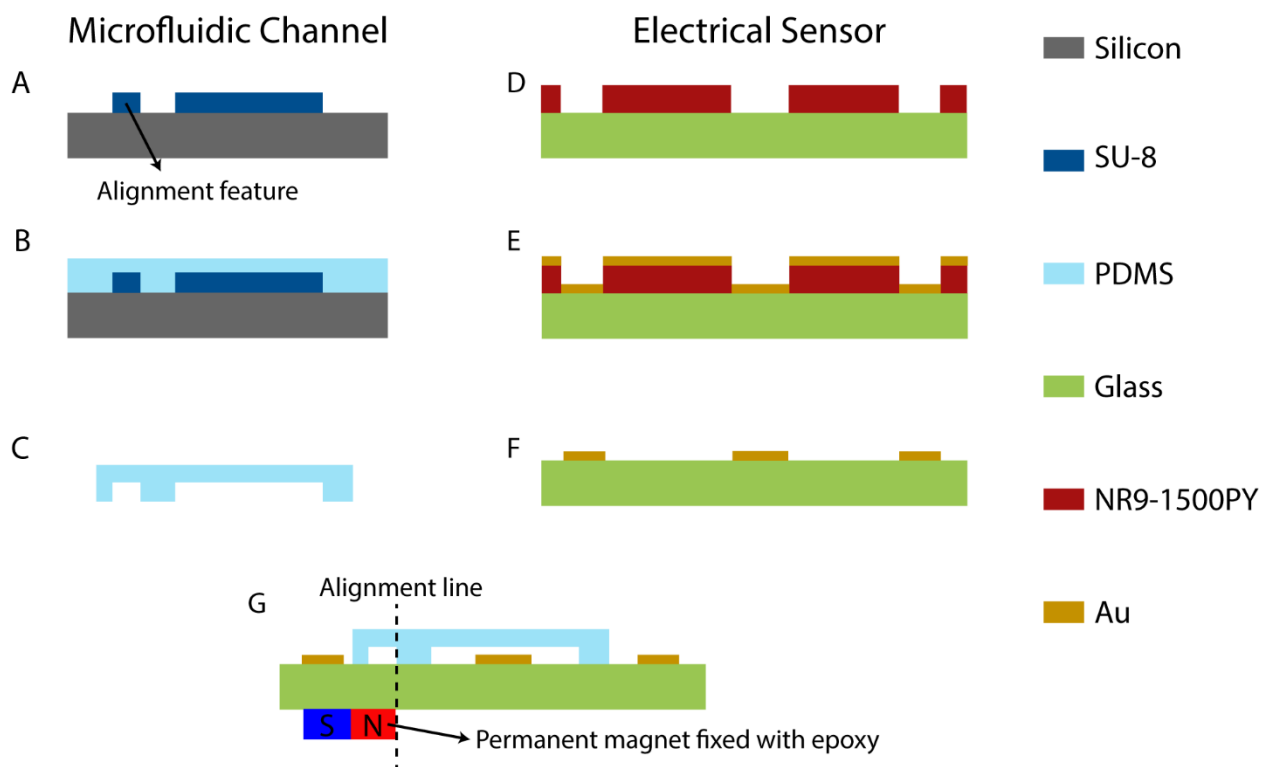

Fig. S1 Fabrication process. SU-8 photoresist was spun onto a 4-inch silicon wafer and patterned using photolithography. 10:1 mixture of PDMS and crosslinker was poured onto the wafer, degassed and cured. Then, the PDMS was peeled off and sliced into individual devices. For electrode fabrication, NR9-1500PY photoresist was spun onto a 1 by 3-inch glass slide and patterned using photolithography. Au/Cr film stack was deposited onto the substrate using an e-beam evaporator, and lift-off is performed. The layers were treated under oxygen plasma for surface activation, aligned under a microscope and bonded together. Finally, the permanent magnet was aligned under a microscope and fixed to its position by epoxy.
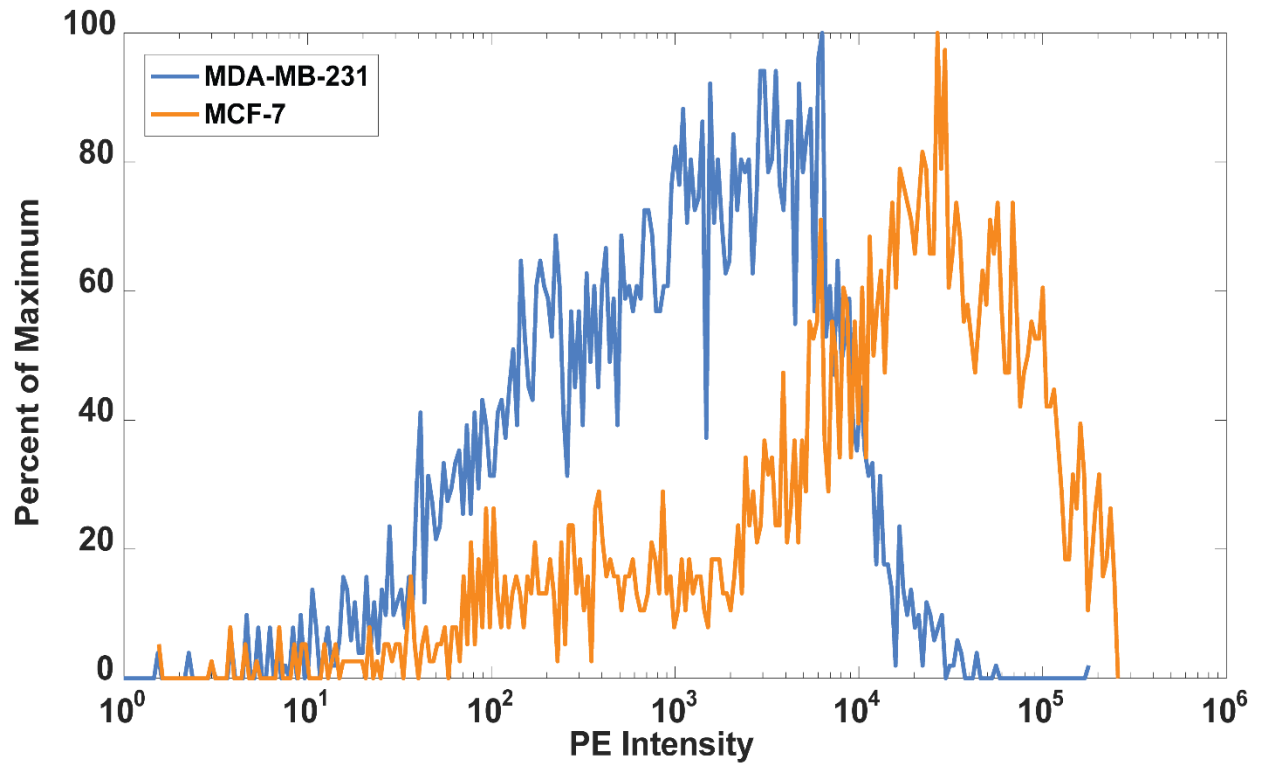
Fig. S2 Flow cytometry measurement of MDA-MB-231 and MCF-7 breast cancer cells that were labeled with PE conjugate anti-EpCAM antibody (Methods). MCF-7 cells showed higher mean EpCAM expression than MDA-MB-231 cells.
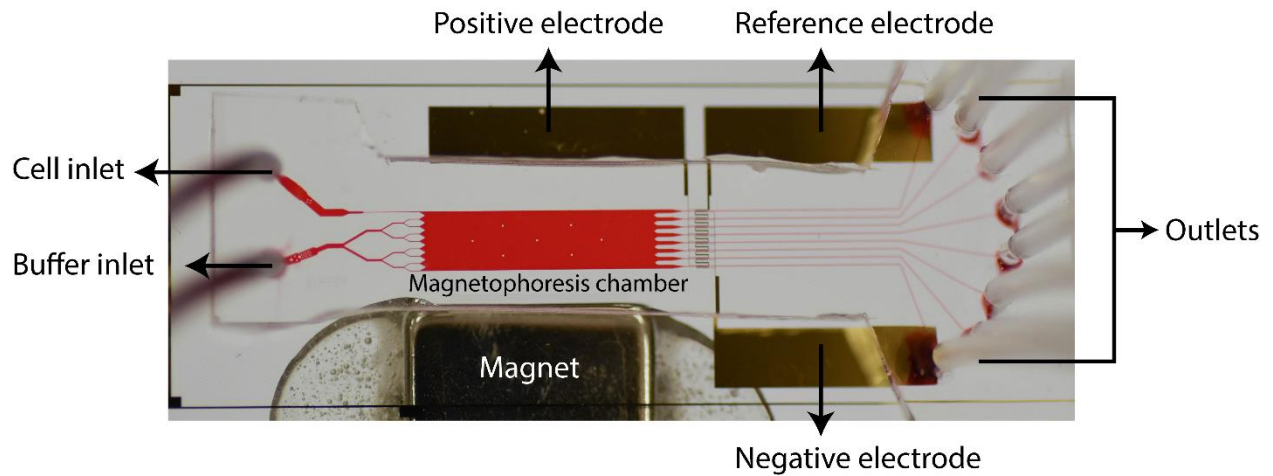
Fig. S3 A photo of the analytical version of the microfluidic device used to microscopically characterize cells sorted into individual microfluidic bins. Cells were independently collected from eight microfluidic bins via dedicated outlets and subsequently analyzed via fluorescence microscopy.
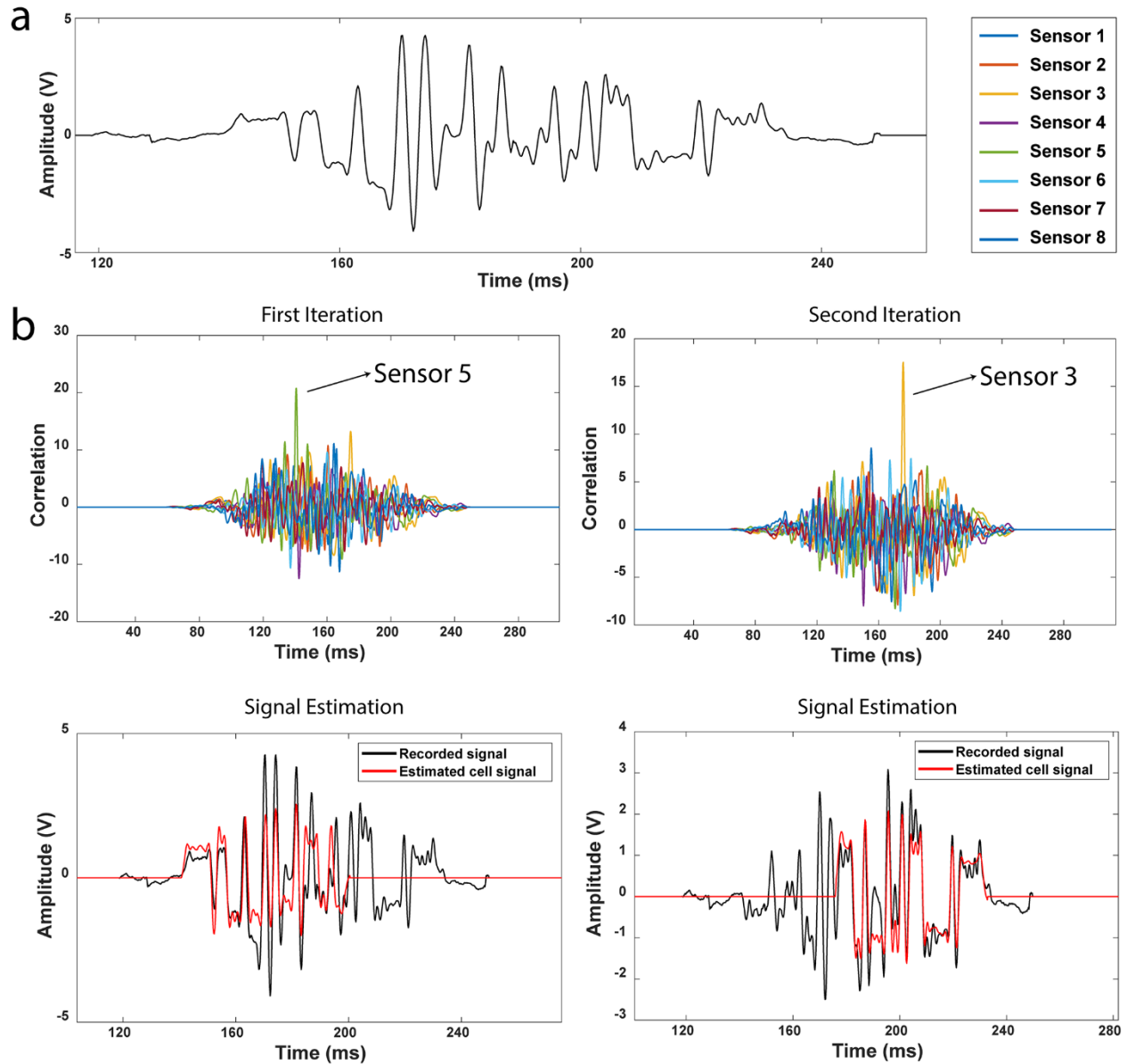
Fig. S4. (a) An output waveform due to two sorted cells coincidently interacting with the electrical sensor. The signal results from the interference of two signals coming from microfluidic bins #3 and #5. (b) Decoding of the waveform using successive interference cancellation. In the first iteration the signal corresponding to the larger cell was estimated using the highest correlation value and the estimated waveform was subtracted from the original signal to cancel its interference. The process was repeated to identify remaining sensor signals until the residual signal did not produce a correlation above a set threshold.
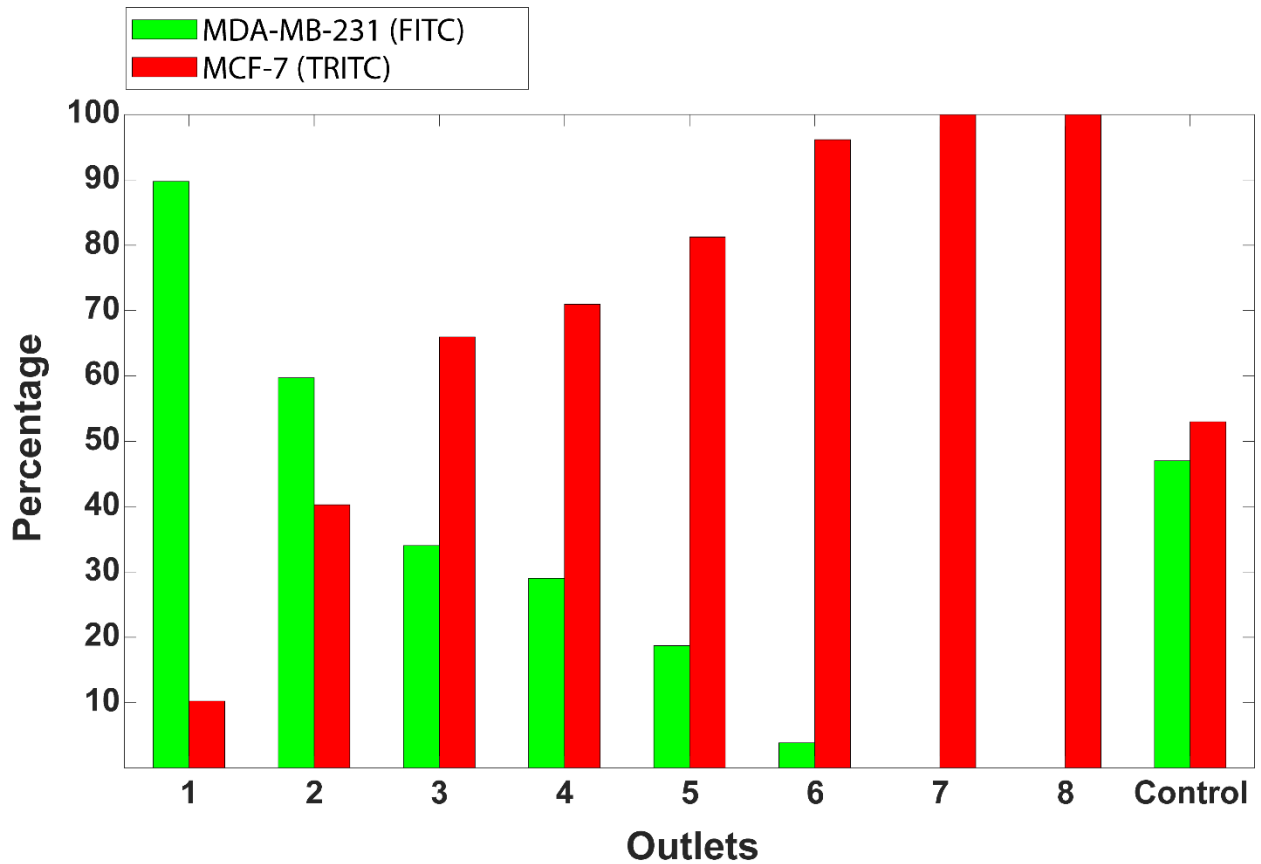
Fig. S5 Fluorescence microscopy characterization of cell populations sorted into each microfluidic bin from processing of a 1:1 mixture of FITC-labeled MDA-MB-231 cells and TRITC-labeled MCF-7 cells. Sorted populations were collected from individual microfluidic bins and were imaged together with the unprocessed sample. Low expressor MDA-MB-231 cells constituted the majority in the closer bins while the high expressor MCF-7 cells gradually became more prevalent in distant bins as these cells could deflect more under the same magnetic field based on their higher magnetic load compared to MDA-MB-231. Control bars show the fractions of two cell lines in the sample prior to processing.
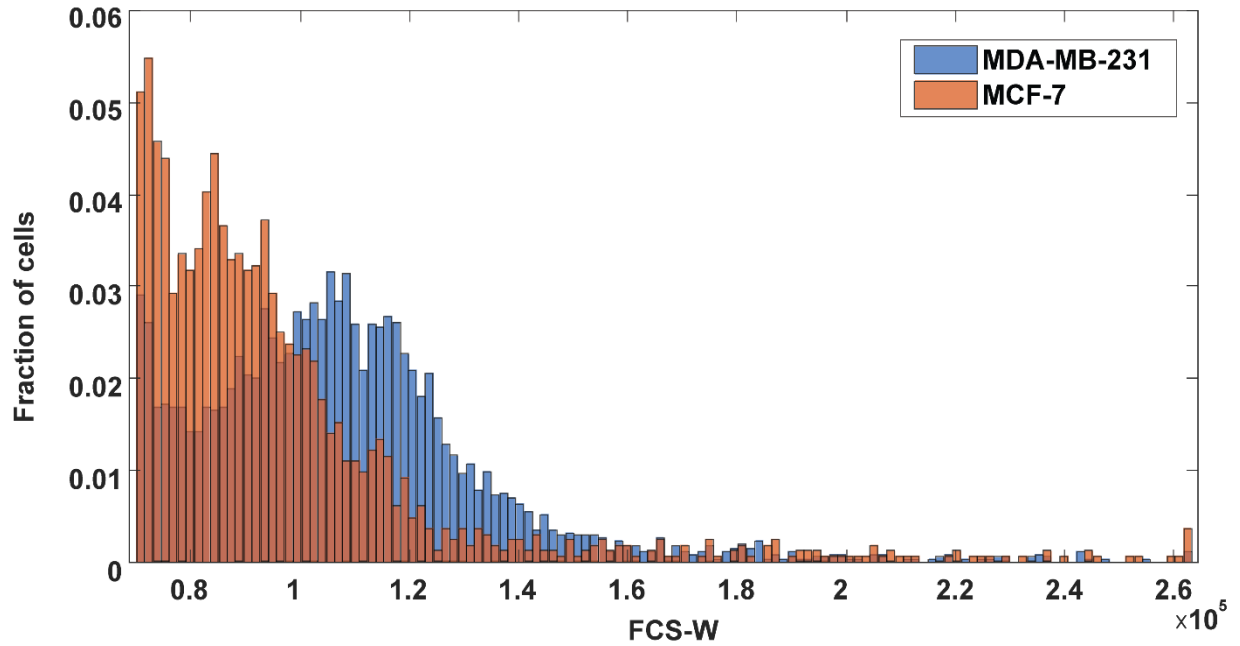
Fig. S6 Analysis of cell size for MDA-MB-231 and MCF-7 cell lines via flow cytometry. Forward scatter width data from the cytometer were used to analyze the cell size as it correlates linearly with the cell size[3]. The analysis showed that MDA-MB-231 cells were larger and had a wider spread in size than MCF-7 cells.
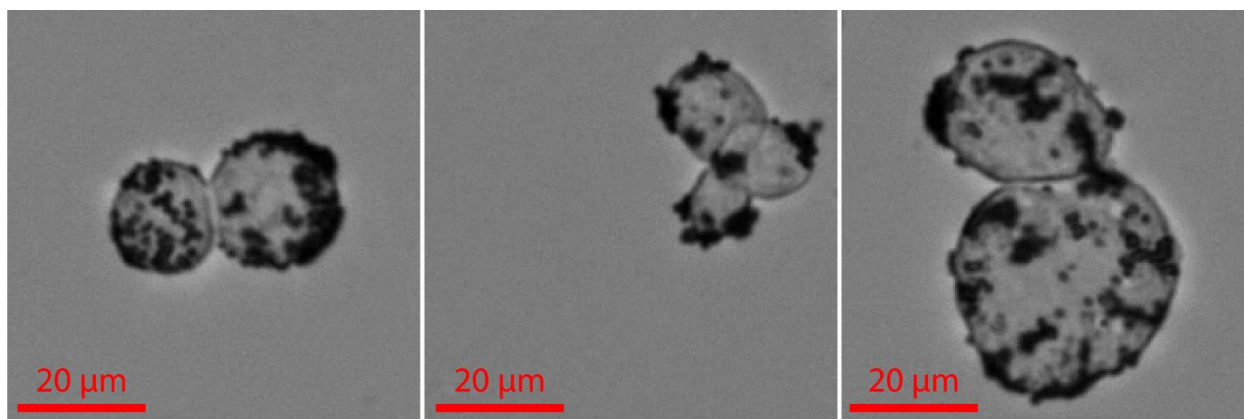
Fig. S7 Microscope images of immunomagnetically labeled clumped SK-BR-3 cells. Clumped cells were identified in the electrical data from larger signal amplitudes they produced compared to single cells.

Fig. S8. Automatic quantification of a cell magnetic load from microscope images. Images of the cells were taken at 20X and the morphological operations were made on the image to create a binary map with enhanced contrast between the magnetic beads and the background. The number of magnetic beads was computed from the calculated area occupied by the magnetic particles.

Table S1 | 31-bit Gold sequences.

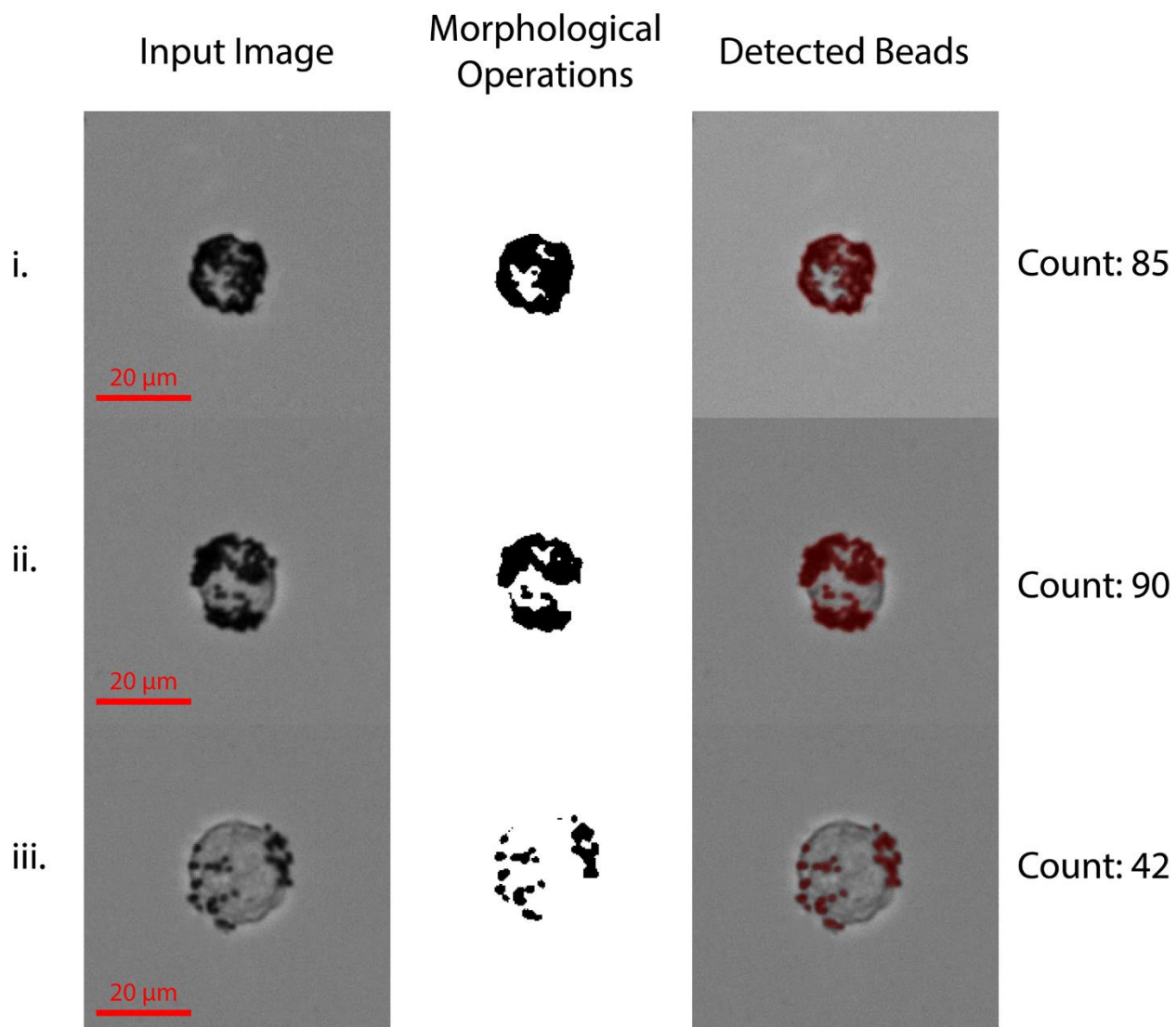| Code index	31-bit Gold Code	Implementation
1	1 0 1 0 1 1 1 0 1 1 0 0 0 1 1 1 1 1 0 0 1 1 0 1 0 0 1 0 0 0 0	Bin 1
2	1 0 1 1 0 1 0 1 0 0 0 1 1 1 0 1 1 1 1 1 0 0 1 0 0 1 1 0 0 0 0	Bin 2
3	0 0 0 1 1 0 1 1 1 1 0 1 1 0 1 0 0 0 1 1 1 1 1 1 0 1 0 0 0 0 0	Bin 3
4	1 1 1 0 1 0 0 0 1 0 0 1 0 0 1 0 0 1 1 0 1 0 0 0 0 0 1 0 0 0 1	
5	0 0 0 0 1 1 1 0 0 0 0 0 0 0 1 0 1 1 0 0 0 1 1 0 1 1 1 0 0 1 0	
6	1 1 0 0 0 0 1 1 0 0 1 0 0 0 1 1 1 0 0 1 1 0 1 1 0 1 1 0 1 0 1	Bin 4
7	0 1 0 1 1 0 0 1 0 1 1 0 0 0 0 1 0 0 1 0 0 0 0 0 0 1 1 1 0 1 0	
8	0 1 1 0 1 1 0 1 1 1 1 0 0 1 0 0 0 1 0 1 0 1 1 0 0 1 0 0 1 0 1	
9	0 0 0 0 0 1 0 0 1 1 1 0 1 1 1 0 1 0 1 1 1 0 1 0 0 0 1 1 0 1 1	Bin 5
10	1 1 0 1 0 1 1 0 1 1 1 1 1 0 1 1 0 1 1 0 0 0 1 0 1 1 0 0 1 1 1	
11	0 1 1 1 0 0 1 0 1 1 0 1 0 0 0 0 1 1 0 1 0 0 1 1 0 0 1 1 1 1 0	Bin 6
12	0 0 1 1 1 0 1 0 1 0 0 0 0 1 1 1 1 0 1 1 0 0 0 0 1 1 0 1 1 0 1	
13	1 0 1 0 1 0 1 0 0 0 1 0 1 0 0 1 0 1 1 1 0 1 1 1 0 0 0 1 0 1 1	
14	1 0 0 0 1 0 1 1 0 1 1 1 0 1 0 0 1 1 1 1 1 0 0 0 1 0 0 0 1 1 0	
15	1 1 0 0 1 0 0 1 1 1 0 0 1 1 1 1 1 1 1 0 0 1 1 1 1 0 1 1 1 0 0	
16	0 1 0 0 1 1 0 0 1 0 1 1 1 0 0 1 1 1 0 1 1 0 0 1 1 1 0 1 0 0 0	Bin 7
17	0 1 0 0 0 1 1 0 0 1 0 1 0 1 0 1 1 0 1 0 0 1 0 1 0 0 0 0 0 0 1	
18	0 1 0 1 0 0 1 1 1 0 0 0 1 1 0 1 0 1 0 1 1 1 0 0 1 0 1 0 0 1 1	
19	0 1 1 1 1 0 0 0 0 0 1 1 1 1 0 0 1 0 1 0 1 1 1 1 1 1 1 0 1 1 1	
20	0 0 1 0 1 1 1 1 0 1 0 1 1 1 1 1 0 1 0 0 1 0 0 1 0 1 1 1 1 1 1	
21	1 0 0 0 0 0 0 1 1 0 0 1 1 0 0 0 1 0 0 0 0 1 0 0 0 1 0 1 1 1 1	
22	1 1 0 1 1 1 0 0 0 0 0 1 0 1 1 1 0 0 0 1 1 1 1 0 0 0 0 1 1 1 0	
23	0 1 1 0 0 1 1 1 0 0 0 0 1 0 0 0 0 0 1 0 1 0 1 0 1 0 0 1 1 0 0	
24	0 0 0 1 0 0 0 1 0 0 1 1 0 1 1 0 0 1 0 0 0 0 1 1 1 0 0 1 0 0 1	
25	1 1 1 1 1 1 0 1 0 1 0 0 1 0 1 0 1 0 0 1 0 0 0 1 1 0 0 0 0 1 1	
26	0 0 1 0 0 1 0 1 1 0 1 1 0 0 1 1 0 0 1 1 0 1 0 1 1 0 1 0 1 1 0	
27	1 0 0 1 0 1 0 0 0 1 0 0 0 0 0 0 0 1 1 1 1 1 0 1 1 1 1 1 1 0 1	Bin 8
28	1 1 1 1 0 1 1 1 1 0 1 0 0 1 1 0 1 1 1 0 1 1 0 1 0 1 0 1 0 1 0	
29	0 0 1 1 0 0 0 0 0 1 1 0 1 0 1 1 1 1 0 0 1 1 0 0 0 0 0 0 1 0 0	
30	1 0 1 1 1 1 1 1 1 1 1 1 0 0 0 1 1 0 0 0 1 1 1 0 1 0 1 1 0 0 1	
31	1 0 1 0 0 0 0 0 1 1 0 0 0 1 0 1 0 0 0 0 1 0 1 1 1 1 0 0 0 1 0	
32	1 0 0 1 1 1 1 0 1 0 1 0 1 1 0 0 0 0 0 0 0 0 0 1 0 0 1 0 1 0 0	
33	1 1 1 0 0 0 1 0 0 1 1 1 1 1 1 0 0 0 0 1 0 1 0 0 1 1 1 1 0 0 0	

31-bit Gold sequences were generated using polynomials x^5+x^3+1 and $x^5+x^3+x^2+x+1$ with the initial states of "10000". The codes implemented in our device are shown in red.